

This is the manuscript for the paper that Dr. Allred and I have been working on, with help from Merlin Hart and Kendall Mitchell. We will submit this to be peer reviewed in coming weeks.

Retardation of the oxidation of aluminum thin films in low-oxygen and cryogenic environments

Donovan K. Smith, Kendall Mitchell, S. Merlin Hart, and David D. Allred
Department of Physics and Astronomy, Brigham Young University, Provo, UT USA 84602

ABSTRACT

Aluminum is the best choice of materials for coating broadband mirrors. Comparative studies of optical instruments containing aluminum-coated mirrors can be challenging because aluminum oxidizes so quickly in air. Fluoride capping layers have been used to prevent oxidation, but they also decrease the range of high reflectance in the far UV. Aluminum's rapid oxidation is an obstacle to making successive, reproducible measurements, making joint work between laboratories more difficult. In this experiment we studied the effects of storage in cryogenic (liquid nitrogen, hexane, and liquid oxygen) and low-oxygen (dry ice and argon) on the retardation of the oxidation of the aluminum mirrors. We observed that all storage conditions that we tested slowed oxidation by two orders of magnitude. While more work is needed to quantify the retardation effects more specifically, especially for hexane and argon, our data suggests that any of these environments could prove useful in mitigating aluminum oxidation during storage.

Keywords: mirror storage, space telescope mirror, far ultraviolet, spectroscopic ellipsometry, oxidation, longevity.

1. INTRODUCTION

Aluminum (Al) is the most promising candidate for coating next generation, broadband mirrors because of its unmatched high reflectance from far ultraviolet (FUV), through the visible and infrared (IR) wavelengths[11]. Many of NASA's proposed projects, including, for example, the Large UV/Optical/IR Surveyor (LUVOIR) and the Habitable Exoplanet Observatory (HabEx), depend on being able to observe a wide spectrum of electromagnetic radiation [DECAL]. More specifically, these two projects need mirrors that are able to observe further into the Lyman ultraviolet range (LUV, 91.2 nm – 121.6 nm) than legacy technology allows. While other barrier layers have been examined, metal fluoride protective layers are used to prevent oxidation of the aluminum[C60]. Each has a characteristic wavelength below which they are opaque. Mirrors on the Hubble Space Telescope (HST) consist of a 25-nm magnesium fluoride (MgF_2) protective layer over Al. This keeps the reflectance above 115 nm high but causes the mirror's reflectance to drop to around 15% at wavelengths below 110 nm [1]. Since a telescope uses multiple mirrors in series the true reduction of light intensity to the detector can be more than a factor of 100.

These fluoride protective layers are used to combat the oxidation of Al thin films which occurs almost immediately when bare Al is exposed to air. Even a thin layer of aluminum oxide (Al_2O_3) decreases the Al mirror's reflectance in the UV range[13]. It is calculated that a 1 nm layer of Al_2O_3 will decrease the reflectance of the mirrors from 90% (unoxidized) to 20% (1 nm oxide) below 150 nm wavelengths [2]. This is an issue because before the mirrors are launched into space, they will be stored in air for long periods of time. Thus, they will necessarily have protective fluoride overcoats. But how thick must those overcoats be? Our group has experience in studying the oxidation of aluminum under ultrathin fluoride coatings, including aluminum fluoride (AlF_3)[2-8]. If ultrathin fluoride films could be made sufficiently perfect they might be suitable for LUV applications. [5], [6] However, at the present the aluminum under such coatings does oxidize, albeit at a much slower rate than bare aluminum.[Allred2017],[Turley],[Johnson2021]. It would be helpful to find ways to store samples for the purpose of shipping them from one lab to another without them changing significantly and to store them in the lab for future reference. It is also desirable to find ways of storing the samples that allow for a thinner fluoride capping layer. For instance, it is proposed that a 2-3 nm layer of AlF_3 may provide better reflectance in the FUV than current telescopes allow [Hennesy2016]. Better storage conditions will likely make thinner capping layers more viable. Because the coatings significantly retard the growth of the oxide, and because we are investigating means of further retarding the oxidation, we perform all of our experiments herein without a fluoride barrier layer. This helps us to isolate the benefits of the storage without the barrier layer confounding our measurements. Three of the environments studied were cryogens: liquid nitrogen, liquid oxygen, and dry ice, and two

were room-temperature attempts to exclude oxygen and water: liquid hexane and argon gas. We chose to include liquid oxygen to attempt to isolate the cryogenic retarding effect of storage, even in oxygen rich environments.

2. EXPERIMENTAL METHODS

2.1 Deposition of Al samples

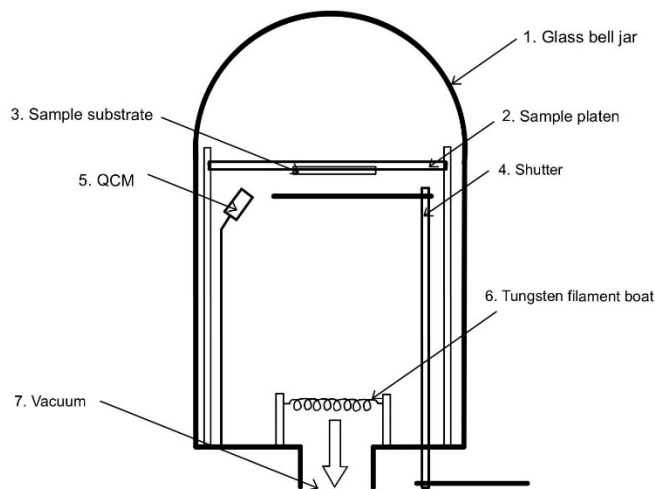


Figure 1: Evaporation Chamber. 1: Bell jar vacuum chamber. 2: Platen which substrates can be attached. 3: Multiple sample substrates are attached facing downwards on the platen. 4: Shutter used to cover the samples to control deposition thickness. 5: Quartz crystal thickness monitor. 6: Al wire is placed in tungsten coil connected to high current power supply. 7. Vacuum pumping system consists of a cryostat pump backed by a mechanical roughing pump.

The aluminum mirror samples were deposited in a Veeco glass bell-jar, thermal evaporator. The evaporator was equipped with an Inficon quartz-crystal thickness monitor (QCM) (labeled 5 in Fig. 1) to measure film thickness during deposition. A sample platen (labeled 2 in Fig. 1) is located about 30 cm above the evaporation source. The platen is drilled with an optical breadboard-like pattern. Threaded holes spaced an inch apart in a square pattern facilitate the attachment of the downward-facing samples to its underside. The platen and samples cannot be rotated. The approximate 30 mm by 30 mm rectangular substrates were cleaved from a 200 mm diameter Si (100) wafer coated with a nominal 300 nm of CVD Si_3N_4 . The CVD Si_3N_4 dielectric layer on the substrate is referred to as the interference layer (IL) and was useful in determining the thickness of the Al and its oxidation in some cases. (reference Allred 17 and Johnson 19-20) The cleaved samples were fixed directly to the 40-cm diameter sample platen with screws and washers. A shutter is placed immediately below the substrate platen (labeled 4 in Fig. 1). It is controlled by a vertical rod attached to a rotational feedthrough in the base plate. In its closed position, it blocks atoms from the evaporation source, while in its open position, it allows atoms to reach the samples attached to the bottom of the substrate platen. Aluminum was evaporated from 99.9% pure Al wire inserted in a 14-turn tungsten coil (RD Mathis) (labeled 6 in Fig. 1). The target Al evaporation rate was 3-4 nm/sec. Since multiple storage environments were investigated, multiple sample sets were deposited. The Al thicknesses ranged between 8 and 80 nm. The chamber was evacuated to below 1×10^{-3} Pa before evaporation. After deposition, the chamber was promptly vented using dry nitrogen gas and the samples were removed for ellipsometric measurement and storage. This time from venting to storage was between 15 and 45 minutes.

2.2 Sample storage

Our initial tests focused on determining the effect of storage in one cryogenic environment (liquid nitrogen) and one water-excluding environment at room temperature (liquid hexane). These studies showed that both environments markedly slowed the formation of aluminum oxide. As a result we added two additional cryogenics (liquid oxygen and dry ice) and one low oxygen environment at room temperature (argon) as test environments.

2.2.1 Samples storage in cryogenics: liquid nitrogen, liquid oxygen and dry ice

To separate the effect of low-oxygen storage from the effect of low-temperature storage we prepared additional stored samples in a high-oxygen cryogen. We termed this liquid oxygen though no effort was made to completely exclude nitrogen from the mixture. Nor was air rigorously excluded from the liquid nitrogen which is why it is termed low-oxygen rather than oxygen-free cryogenic storage. The liquid oxygen was produced by bubbling research-grade O₂ (purity 99.999%) gas into a Dewar of liquid nitrogen until the mixture reached a temperature of >89K (greater than 95% O₂). Since the normal boiling point of oxygen is substantially higher than that of liquid nitrogen (90 versus 77 K) liquid oxygen replaces nitrogen in the cryogenic mixture. At this point the liquid took on a profound blue color. The volume of liquid cryogen substantially decreased during the condensation process. After a quantity of liquid oxygen was produced in the production Dewar, it was transferred to the test Dewar which held the samples. In the case of both liquid N₂ and liquid O₂ the samples were held in commercial dippers which came with the 10-liter dewars. The design allowed up to six dippers with multiple samples to be stored in the liquid cryogen. The dippers allowed for the easy storage and retrieval of specific samples. For measurements, the dipper was brought to the neck of a Dewar so that a sample could be removed while avoiding warming the rest of the samples. Because the cryogenics slowly turned into gas and escaped the dewars, we checked at regular intervals, typically 2 – 4 days, and added more cryogen as needed to keep the samples well covered.

We also wished to test whether an easier-to-transport cryo-environment (Dry ice storage) would similarly retard oxidation. Each batch of samples that was created during the same run of the evaporator were labeled in storage so time in storage could easily be determined. Dry ice storage consisted of a Styrofoam insulated cold-shipping box in which the samples were stored in a glass beaker surrounded by dry ice. The samples were separated from one another by dividers. An aluminum foil lid was used to reduce the amount of dry ice that contacted the samples directly. Dry ice evaporation was more rapid than for the liquid cryogen and the storage container was refilled with dry ice several times each week.

When samples were removed from cryogenic conditions, condensation could form on the surface of the cold samples. Even though ambient lab air was dry, with relative humidity of 18 to 22%, this corresponds to a dewpoint of 270 to 273K. The higher humidity levels occurred in summer and the lower ones in winter. In order to minimize frost formation dry-ice stored samples were warmed up on a resistive heater mounted in the mouth of the Styrofoam dry ice container so that they could be warmed to ambient temperatures in a semilow oxygen environment. This greatly reduced the amount of condensation formed on the samples and the time it stayed on the sample. After variable-angle, spectroscopic ellipsometry (VASE) measurements, samples could be returned to storage, however, eventually samples were left in lab conditions out of storage so that the samples could act as their own control sample. For each sample, we were able to compare the in-storage change in oxide thicknesses to the change in the sample with time while the sample was in ambient lab-air conditions.

Storing the samples in this way can provide a clear picture of the differences between storage in special environments- i.e., cryogenic and low-oxygen environments and storage in ambient air conditions at room temperature.

2.2.2 Storage at room-temperature: samples stored in liquid hexane and samples in argon gas.

Some of the samples prepared for the initial study were stored in hexane. No attempt was made to “degas” the hexane by bubbling in an inert gas such as N₂. In order to more fully observe viable storage environments for aluminum mirrors, another non-cryogenic candidate was investigated. Argon gas is cheap, and inert, and with the added benefit that one can store mirror samples at room temperature in a sealed container.

After initial measurements via VASE, five Al coated samples were placed in a low-oxygen (< 0.5 ppm) argon-filled glove box. While in the glove box, each was sealed in a separate glass jar. The jars were heated on a hot plate until they reached ~100° C, then canning lids and rings were placed on them. These lids have a rubber seal. When the jars with samples in side were removed from the hot plate the air inside the jars cooled, creating a pressure difference, sealing the jar. Four of the sealed jars were then removed from the argon box and the jars were kept in ambient lab air. The fifth jar remained in the glove box for the duration of its storage time. Because we needed to break the seal to make measurements of these samples, once a sample was removed it remained in ambient lab air for subsequent measurements as time elapsed.

Because the sample would be sealed with an impurity of < 0.5 ppm oxygen, we expected to see negligible oxidation of the samples stored between the first measurement pre-seal and second measurement after taking the sample out of storage.

2.4 Ellipsometric characterization and oxide thickness determination.

Samples were characterized via VASE over the 193-1690 nm wavelength range using a JA Woollam M2000. Later samples were measured using a Woollam RC-2 over a range of 191- 1000 nm. Ellipsometric data were then modeled using the CompleteEASE® software from J.A. Woollam Company to extract thicknesses.

The top layer of the model is alumina, aluminum oxide. It is the thinnest of the layers since it is not deposited but grows from the oxidation of the aluminum layer. Since it is so thin, the first approach examined was to use literature optical constants for sapphire, also termed, corundum. However, sapphire optical constants produced poor fits to the data with large mean square error and an unphysically thick alumina layer[Johnson 2021]. In addition, the apparent layer thicknesses would vary randomly between subsequent measurements. Instead, the Al_2O_3 was parameterized as a Cauchy layer, with fit parameters from previous work. This is defensible since the alumina that forms is likely not corundum/sapphire and can be expected to have different optical constants. The thicknesses calculated for the oxide layer as part of the as-deposited sample yield consistent results even as samples aged. Nevertheless, the UV optical constants were not completely satisfactory. The modeled fits to the ellipsometric parameters, psi and delta, showed notable deviations between measured and modeled data at shortest wavelengths.

Under the alumina layer, lay the deposited Al film. The optical constants for thin-film metal layers like Al need to be treated differently than dielectrics because their optical constants depend on the behavior of their free electrons. These in turn are thought to depend on film thickness, grain sizes and deposition conditions. This has long been known to be the case for aluminum [Nguyen1993]. In the present study, the Al layer was modeled as the sum of four to six Gaussian oscillators, a UV pole and the value of the dielectric constant at large energy. The oscillator at zero eV corresponds to the free electron (Drude) contribution to aluminum's conductivity. The intensity and breadth of this oscillator varies with the thickness of the film and deposition conditions such as impurity concentration. For each sample studied, we fit the Al parameters and kept them constant or that sample as it aged.

It was recognized, however, that an effective medium approximation (EMA) layer could be helpful for understanding aging. Ultrathin aluminum films are known to have many grain boundaries, conceivably oxygen could penetrate along them, producing a small amount of oxide in the interior of the layer. Previous investigation had not found evidence of this in the oxidation of Al under MgF_2 . [allred -17] Nevertheless, we investigated this possibility for bare aluminum by replacing the aluminum layer with an EMA layer composed of Al with voids and a small amount of aluminum oxide.

Beneath the aluminum layer was a layer of approximately 300 nm of silicon nitride (Si_3N_4) and beneath it, the Si wafer. The silicon nitride layer allowed for thin-film interference when the Al layer was sufficiently thin. This has been shown to facilitate the determination of the indices and thickness of absorber layers like the aluminum.[Hilfike2008]. The thickness of this layer is set to a nominal 300 nm for the first part of fitting each sample, and then once the thickness of the other layers converge, its thickness was fit. The thickness of the nitride did not vary by more than about 3% from the initial estimate. Silicon wafers generally have 1 to 2 nanometer of native oxide and we included a silicon dioxide (SiO_2) layer with a nominal 1nm thickness. We did not find that allowing this to fit had any great effect on our MSE, so we held it constant.

For some of the samples studies, the deposited Al was opaque and no interference fringes could be seen. For thicknesses of Al > 40 nm, most of the incident light is absorbed or reflected and no evidence of interference fringes from the underlying silicon nitride could be seen. In such case, the layers underneath the Al were ignored.

2.5 Data Analysis

It has been noted that that the growth in the apparent oxide thickness on aluminum slows down dramatically as the thickness of the oxide already on the film increases. Several approaches to parameterizing thickness with time-in-air have been examined for room temperature oxidation including linear, parabolic, inverse-logarithmic (that is, Cabrera-Mott), and logarithmic. Al oxide thickness increases linearly with the logarithm of time [Brian Johnson]. That is, when apparent thickness is plotted versus the logarithm of time, the thickness values lie more-or-less on a straight line.

After the data were analyzed using CompleteEASE®, thickness versus time plots were generated via python and the retardation factor of each storage environment was determined. The growth for oxide on an aluminum thin film typically

follows a logarithmic trend [BYU ones (2-6)]. We used the following piecewise logarithmic function for fitting the retardation factor. In this equation, 'Th(t)' is the thickness of the aluminum oxide, 's' the slope of the thickness vs. log time graph, 't' is the time in hours since deposition, 'st' is the storage time in hours, 'rf' is the retardation factor, 'y0' is the computed value for the oxide thickness at one hour after the sample was removed from the deposition chamber, and 'TOF' is the time offset in hours.

$$Th(t) = \begin{cases} s * \ln(t * rf) + y0 & t \leq st \\ s * \ln(t - TOF) + y0 & t > st \end{cases} \quad (\text{Eq 2.1})$$

The retardation factor is defined below such that Eq 2.1 is continuous at $t = st$:

$$rf = 1 - \frac{TOF}{st} \quad (\text{Eq 2.2})$$

This bounds the rf between 0 and 1 because the maximum allowed TOF is the storage time st. In other words, the TOF is the amount of time in storage that, from the sample's perspective, seems not to have elapsed because of the storage. To obtain TOF we fit the data to Eq 2.1 with nonlinear least squares procedure for each of 20 equally spaced TOF trial values between 0 and the total storage time. For each of these values, we determined the coefficient of determination, R². An example is shown in Fig. 2 We decreased the mesh near the maximum value until we had the highest value of R², and that TOF was used in Eq 2.2. to obtain the retardation factor. A demonstration of the step-by-step calculation of rf is discussed in the next section.

3. RESULTS AND DISCUSSION

The questions motivating our investigation were these: does storage in low oxygen environments retard oxidation? Does cryogenic storage retard oxidation? We define the *retardation factor* as the ratio of the amount of time needed for oxidation in air to the equivalent time in a storage condition to achieve the same oxide thickness. For instance, if 1 nm of oxide formed in air in 30 minutes, and that same 1 nm of oxide took 30 hours to form on a sample in storage, then that storage media would be assigned a retardation factor of 1/60 because the oxidation happened 60 times more slowly in storage.

Summarizing, the retardation factors were determined in the following manner. After deposition, samples were immediately measured via VASE. Then all were placed in storage. Except for samples stored in argon, which were not placed back in storage, samples were periodically removed from storage long enough to make measurements (about 5-10 minutes) before being placed back into storage. Eventually a sample was retired from storage and allowed to freely oxidize in air at room temperature. After samples were removed permanently from the storage condition, we continued to measure them. This allowed us to observe the same sample oxidizing both in ambient air conditions and in its respective storage condition. This is important because deposition conditions and each samples' unique topography could affect the subsequent oxidation of the aluminum. By measuring samples both before and after they were in storage, we were able to find a self-consistent ratio of the oxidation of a single sample in two different environments.

3.1 Liquid Nitrogen

To demonstrate the process our fitting procedure, we provide a demonstration with one of our samples that was stored in liquid nitrogen. Figure 2 shows the thickness of the aluminum oxide plotted against the time since deposition. It is clear that the point measured before storage and the points measured after storage do not fit on the same line. The goal of the fitting procedure is to adjust the time values by finding a retardation factor that puts all of the points from after storage on the same line as the points taken before and during storage. Figure 3 shows the plot of coefficient of determination of the points on the logarithmic line. This figure shows that the goodness of the fit is strongly dependent on the offset time. The value that we accepted for the offset time for each sample, which was then used to calculate the retardation factor,

was the maximum of this curve. Figure 4 shows the aluminum oxide thickness data for the same sample after the time adjustment has been made.

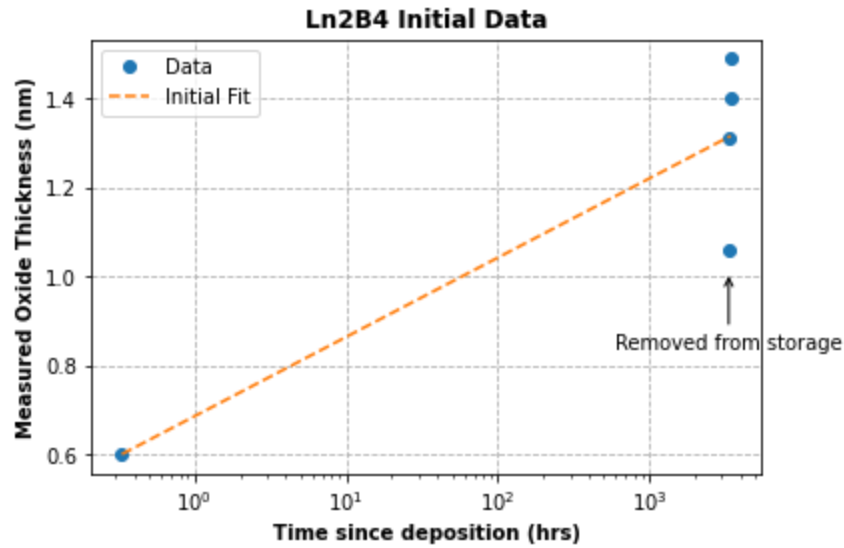


Figure 2: Aluminum oxide thickness vs. Time since deposition for sample B4 stored in liquid nitrogen. There are no time adjustments here. The fit line represents the expected logarithmic oxidation in air. The fact that the points after removal from storage do not fit on the same line as the point before storage is evidence that liquid nitrogen storage retards the growth of aluminum oxide.

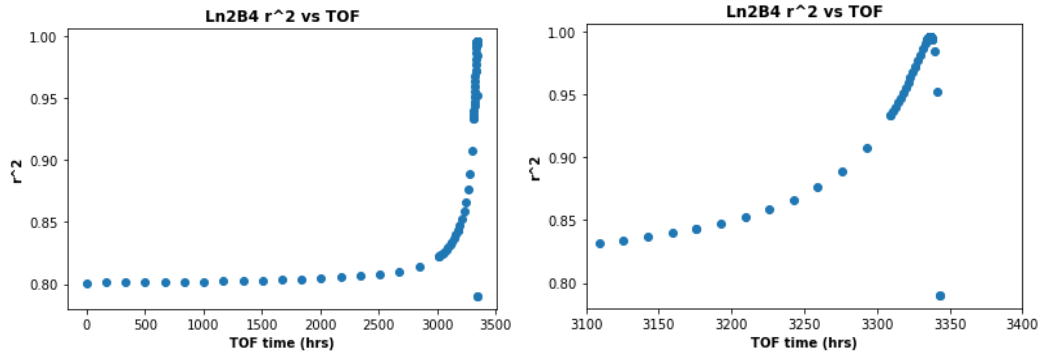


Figure 3: Coefficient of Determination as a function of the offset time, TOF for a sample stored in LN. This demonstrates that thickness function is very sensitive to the value of TOF. The second plot has a smaller range of the same values so that it is easier to see what is going on when the points get closer together.

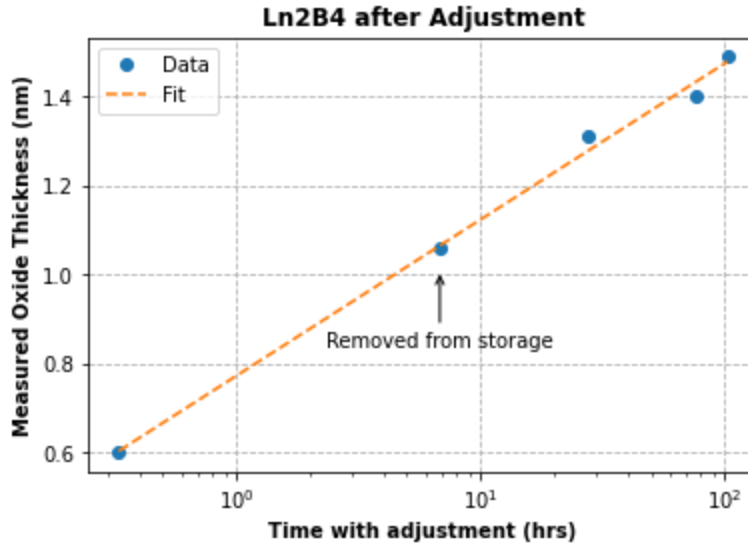


Figure 4: Thickness vs time data for sample B4 stored in liquid nitrogen. The time data has been adjusted here according to equations 2.1 and 2.2. The retardation factor for this sample was 0.00194.

For each of the samples stored in liquid nitrogen, we performed the fit procedure described above, and we found retardation factors ranging between 0.001 and 0.002.

3.2 Hexane

Hexane is a liquid which by in large, excludes water and/or oxygen at room temperature. These are thought to be the two primary actors in the oxidation of aluminum. Thus, hexane is a candidate room temperature medium that may retard aluminum oxidation. Various bare aluminum samples were stored in the hydrocarbon hexane (C_6H_{14}) at room temperature to study the effects of storage in a low-oxygen environment at room temperature. The samples that were stored in hexane were treated as those in LN2 as explained above. We observed retardation factors that had more scatter, between 0.1 and 0.005. While this shows that there is at least an order of magnitude retardation, more work is needed to understand the particular amount of retardation provided by hexane storage.

3.3 Liquid oxygen

Samples stored in liquid oxygen were handled in much the same way as those that were in liquid nitrogen and hexane, however, we include figures 5 and 6 to demonstrate that the fitting procedure that we used also allows for samples to be taken out of storage for measurements before being removed from storage long term. The retardation effects appear to continue even after very brief removal from storage. The retardation factors observed for liquid oxygen storage range from 0.002 to 0.003. While storage in liquid oxygen is not practical for safety reasons, this does indicate that even in the presence of high concentrations of oxygen, cryogenic storage has a strong retarding effect on the growth of aluminum.

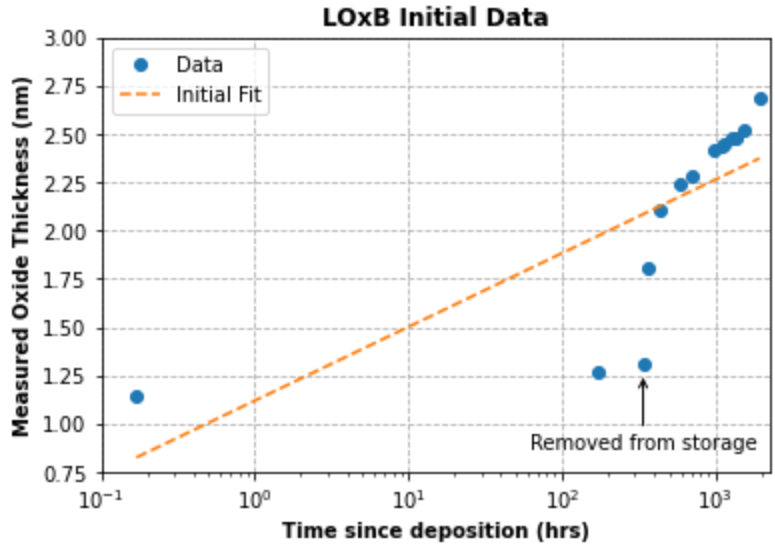


Figure 5: The aluminum oxide thickness data vs log time since aluminum deposition for sample LOx-B, retardation factor = 0.00160 . There are no adjustments in time. The first three data points correspond to oxide thickness just before LOx storage, at one week and at two weeks. The fit line represents the expected logarithmic growth expected for oxidation in air. The fact that the oxide thickness does not fall on a logarithmic plot is indicative of retardation of oxidation for aluminum films stored in LOx.

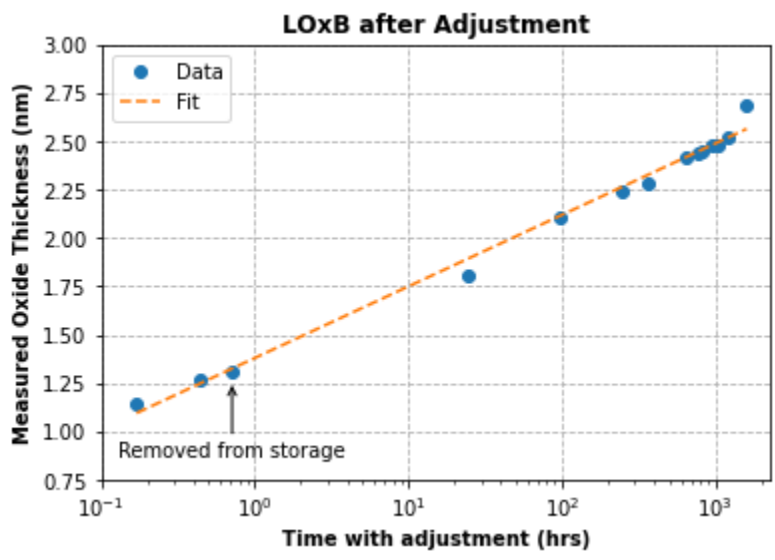


Fig. 6: The data for sample LOx-B, with time adjusted using equations 2.1 and 2.2. The first three data points correspond to oxide thickness as measured just before LOx storage, at one week and at two weeks respectively.

3.4 Dry Ice

Sending samples stored in LN2 or hexane across the country to be analyzed at a different lab could be challenging. Pressurized containers are dangerous and an open container is subject to spilling. This led us to investigate the viability of using dry ice to slow the rate of growth aluminum oxide in our samples because dry ice can be used in shipping and will not spill easily. Our dry ice samples were placed in a dry ice shipping box. The sample was sandwiched between dry ice, with newspaper and lint free cloth isolating the sample from direct contact with the dry ice. Every two to three days the dry ice was replaced. The sample was kept as cold as possible during the refills and the refilling process was done as

fast as possible. The sample was exposed to the atmosphere for less than 2 minutes each time the dry ice was replaced, but was not given the opportunity to warm up. VASE measurements were taken during the storage process. This means the samples were taken from storage, measured and then put back in storage.

The retardation factors that we observed for the samples we had stored in dry ice ranged from 0.001 to 0.007. While this range is large, in all cases, the retardation was two orders of magnitude.

3.5 Argon

Argon provides a potential storage solution which doesn't invoke the use of cryogenics to retard oxygenation. It is expected that in an argon environment with less than 0.5 ppm oxygen, the oxidation rate of aluminum would be greatly diminished. We found that the containers that we used had a large effect on the quality of the oxidation retardation. The samples were sealed inside mason jars while inside low oxygen (0.5 ppm) Argon glove box. One of the jars was left in the glove box, and it had a retardation factor significantly lower than the jars that were stored in air when analyzed as described above. We therefore distinguished samples further as Argon in Argon for the sample that stayed in the glove box the whole time and Argon in air for the samples that were sealed in jars and kept in lab air. The argon in argon sample had a retardation factor of 0.005 while the samples stored in argon in air had retardation factors ranging between 0.03 and 0.1.

We summarize the findings from the several storage conditions in table 1.

Storage Condition	Retardation Factor (10^{-3})	Ratio of air time to storage time
Liquid Nitrogen	1.7 ± 0.49	641 ± 225
Hexane	51 ± 66	112 ± 144
Liquid Oxygen	2.5 ± 0.75	439 ± 161
Dry ice	3.6 ± 2.4	412 ± 277
Argon in Air	86 ± 80	21 ± 19
Argon in Argon	4.5	223

Table 1: The average retardation factor for each of the storage conditions. Cryogenics liquid nitrogen, liquid oxygen, and dry ice performed had the strongest retardation effect (the lowest retardation factor).

4. SUMMARY AND CONCLUSION

Storing freshly deposited, front surface Al mirrors in low-oxygen and/or cryogenic environments is observed to retard the growth of oxide by more than two orders-of-magnitude. The retardation factor was defined as the ratio of time that a change would have taken in open dry air (20% RH) at room temperature divided by the elapsed time storage time. Variable-angle, spectroscopic ellipsometry was used to measure the samples before, during and after storage. A total of 16 samples were stored in five different environments. We subsequently modelled the apparent growth of aluminum oxide on each of the aluminum thin-film samples. The initial thickness of the oxide and the aluminum optical constants were modelled using multi-sample analysis for all measurements of a given sample. The optical constants of the oxide were not modeled due to the thinness of the layer. By comparing the amount of oxide growth on several films in each of the environments, we observed that the oxide growth is retarded by storage in all environments, with the strongest and most consistent effect observed in the cryogenics: liquid nitrogen, liquid oxygen, and dry ice with RF= 0.0017, 0.0025 and 0.004) in that order. The weakest effects, with greatest variability, were observed for samples stored at room-temperature in low-oxygen environments. Specifically, the retardation factor for the two samples stored in hexane at room temperature were 0.1 and 0.005. While the RF for samples stored in argon-filled canning jars was measured to be 0.1 and 0.03. These results on retardation of oxidation could be important for those wishing to maintain front-surface aluminum mirrors stored as references, as well as for those wishing to transport such mirrors to other locations. The

results may also be applicable for mirrors with ultrathin protective coatings which need to be stored for long periods of time though this study would need to be done.

DISCLOSURE

The authors declare no conflicts of interest.

ACKNOWLEDGEMENTS

We would like to thank these Brigham Young University personnel: R. Steven Turley for helpful suggestions interpreting data, Matt Linford for assistance with VASE, John Ellsworth with help on the evaporator used to prepared samples, and Ben Frandsen for use of the low-oxygen glove box. This paper would not have been possible without their help and support. Donovan Smith, Kendall Mitchell, and Merlin Hart received RA support from Brigham Young University, College of Physical and Mathematical Science.

REFERENCES

- [1] Fleming, B., Quijada, M., Hennessy, J., Egan, A., Del Hoyo, J., Hicks, B. A., Wiley, J., Kruczek, N., Erickson, N., and France, K., "Advanced environmentally resistant lithium fluoride mirror coatings for the next generation of broadband space observatories," *Appl. Opt.* 56, 9941-9950 (2017).
- [2] Davis, A. A. "Oxidation of Aluminum Under Various Thicknesses of Aluminum Fluoride," B.S Thesis. Brigham Young University, 2018. <https://physics.byu.edu/library/theses/2018/2>
- [3] Miles, M. "Evaporated Aluminum Fluoride as a barrier Layer to Retard Oxidation of Aluminum Mirrors" Theses and Dissertations, BYU. 6630 (2017). <https://scholarsarchive.byu.edu/etd/6630/>
- [4] Allred, D. D., Turley, R. S., Thomas, S. M., Willett, S. G., Greenberg, M. J., And Perry, S. B., "Adding EUV reflectance to aluminum-coated mirrors for space-based observation," *Proc. SPIE* 10398, 34 (2017).
- [5] Fronk, K.. "Storage of Al/AlF₃ Thin-Film Mirrors in 327 K Oven," B.S. Thesis, Brigham Young University, 2021 <https://physics.byu.edu/library/theses/2021/2>
- [6] Hart, Merlin "Retarding the Growth of Oxide on Aluminum Thin-Films," B.S. Thesis, Brigham Young University, 2022 <https://physics.byu.edu/library/theses/2022>
- [7] Lewis, Devin "Degradation of Lithium Fluoride Mirror Coatings in Humid Environments," B.S. Thesis, Brigham Young University, 2022 <https://physics.byu.edu/library/theses/2021>
- [8] Johnson Brian I., Avval, Tahereh G., Turley, R. S., Matthew R. Linford, M.R., and David D. Allred "Oxidation of aluminum thin films protected by ultrathin MgF₂ layers measured using spectroscopic ellipsometry and X-ray photoelectron spectroscopy." *OSA Continuum* 4 (3), 879-895 (2021).
- [5] Hennessy, J., Balasubramanian, K., Moore, C. S., Jewell, A. D., Nikzad, S., France, K., & Quijada, M. (2016). Performance and prospects of far ultraviolet aluminum mirrors protected by atomic layer deposition. *Journal of Astronomical Telescopes, Instruments, and Systems*, 2(4), 041206. <https://doi.org/10.1117/1.jatis.2.4.041206>
- [6] Egan, A., Fleming, B. T., Wiley, J., Quijada, M., Del Hoyo, J., Hennessy, J., Hicks, B., France, K., Kruczek, N., Erickson, N., "The development and characterization of advanced broadband mirror coatings for the far-UV," *Proc. SPIE* 10397, UV, X-Ray, and Gamma-Ray Space Instrumentation for Astronomy XX, 1039715 (31 August 2017); <https://doi.org/10.1117/12.2274141>
- [7] Nguyen, H. V., An, I., Collins, R W., "Evolution of the optical functions of thin-film aluminum: A real-time spectroscopic ellipsometry study," *Physical Review B* 47, 3947 (1993).
- [8] Grimblot, J. "II. Oxidation of Al Films," *J. Electrochem. Soc.* 129(10), 2369 (1982).
- [9] Turley, R. S., "Bare Aluminum Oxidation," *BYU Sch. Arc.* (22 November 2017); <http://hdl.lib.byu.edu/1877/3993>

[10] Hilfiker, J. N., Singh, N., Tiwald, T., Convey, D., Smith, S. M., Baker, J. H. and Tompkins, H. G., “Survey of methods to characterize thin absorbing films with Spectroscopic Ellipsometry,” *Thin Solid Films*, 516 7979–7989 (2008). <https://doi.org/10.1016/j.tsf.2008.04.060>

[11] J. I. Larruquert, J. A. Méndez, and J. A. Aznárez, **Far-ultraviolet reflectance measurements and optical constants of unoxidized aluminum films**, *APPLIED OPTICS* @ Vol. 34, No. 22 @ 1 August 1995, 4892-4899. 149-155.

[12] José A. Méndez, Juan I. Larruquert, and José A. Aznárez, **“Preservation of far-UV aluminum reflectance by means of overcoating with C60 films,”** *APPLIED OPTICS* y Vol. 39, No. 1 1 January 2000,

[13] R. P. Madden, L. R. Canfield, and G. Hass, “On the vacuum ultraviolet reflectance of evaporated aluminum before and during oxidation,” *J. Opt. Soc. Am.* **53**, 620–625 119632.